Reprinted from: *Mesoscale/Synoptic Coherent Structures in Geophysical Turbulence*, edited by J.C.J. Nihoul and B.M. Jamart

EVOLUTION OF RINGS IN NUMERICAL MODELS AND OBSERVATIONS

E.P. CHASSIGNET[1], D.B. OLSON AND D.B. BOUDRA
Rosenstiel School of Marine and Atmospheric Science, University of Miami,
4600 Rickenbacker Causeway, Miami FL 33149-1098, (USA)

ABSTRACT

Observed properties of rings are compared to rings produced in a two-gyre wind driven circulation model and in a model of the Agulhas retroflection. Their temporal evolution is discussed in terms of structure and translation rate. In both observations and numerical model results, propagation speeds 2 to 5 times faster than of an equivalent isolated eddy (which is of the order of the long Rossby wave speed) were observed. The decay rate of model rings with a lateral viscosity of $330\,m^2s^{-1}$ is found to be faster than in observations. Furthermore, it is observed that the model rings have a coherent structure all the way to the bottom and it seems likely that this may also be the case in real oceanic rings. In the specific case of the model Agulhas ring, the factors influencing its motion and evolution are isolated in a series of subsidiary experiments. It is found that as the ring rounds the tip of Africa, there is only a small influence of the large scale flows on the ring propagation. On the other hand, the presence of the African continent provides an additional westward movement in addition to β. As soon as the ring drifts into the South Atlantic tropical gyre, advection by the large scale flows dominates the ring motion.

1 INTRODUCTION

The temporal evolution of rings has been described in models where isolated vortices are placed on a $\beta-$plane (McWilliams and Flierl, 1979; Meid and Lindemann, 1979) and in several time series field observations (Cheney and Richardson, 1976; Olson, 1980; Olson *et al.*, 1985). There have not been any detailed intercomparisons, however, between these observed rings and the model results, nor have rings produced by gyre scale simulations of the ocean been examined in relation to isolated model rings or observations. The early models used amplitudes of ring layer depth and velocities characteristic of very weak observed rings. Recent primitive equation model experiments have included more realistic ring simulations and thus prompted the comparison made here.

In the following, the properties of model rings created in a square basin and in an idealized South Atlantic/Indian Ocean are compared to rings observed from various western boundary currents. The observations use a diagnostic two-layer model described in full in Olson *et al.* (1985) and Olson and Evans (1986). The diagnostic model, which makes use of the topography of observed thermocline depths, is a close match to the multi-layer quasi-isopycnic coordinate numerical model developed by Bleck and Boudra (1981), which is used in the simulations. Comparisons will be made in terms of ring structure, ring translation, ring parameters (Rossby number, Burger number, *etc.*) and ring energetics. In addition, a number of subsidiary

[1]Present address: NCAR, P.O. Box 3000, Boulder CO 80307-3000, (USA)

experiments help to identify and quantify the primary factors influencing the translation speed and direction of the rings. The final discussion considers both 1) the general similarity of the observed and model rings and 2) the temporal decay in the models and observations in relation to the decay mechanisms at work and the frictional parameterization in the model.

2 DESCRIPTION OF THE MODEL AND EXPERIMENTS

The model used in this paper is the Bleck and Boudra (1981) quasi-isopycnic coordinate, primitive equation model. The behavior of rings formed in a double-gyre square flat bottom basin experiment (referred to as 2G) and in an idealized South Atlantic-Indian Ocean flat bottom basin (referred to as E11) are studied and compared to some observations. Both model configurations are driven by a steady zonal wind stress. The parameters for the experiments are presented in Table 1.

Experiment	Number of layers	Thickness of the layers (m)	g' (ms^{-2})	Bottom drag (s^{-1})	Basin size $km \times km$
2G	3	400	.018	10^{-7}	2000
		1600	.003		×
		3000			2000
E11	3	300	.02		2520
		900	.005		×
		3800			1280
	For both experiments, $\Delta x = 20\,km$.				

Table 1: Parameters of experiments 2G and E11. Blanks indicate no change from the previous experiment.

2.1 Experiment 2G

The applied wind stress is

$$\tau_x = -\tau_m \cos(\frac{2\pi y}{L}) \tag{1}$$

where $\tau_m = 1 \times 10^{-4} m^2 s^{-2}$ and $L = 2000\,km$. The resulting circulation pattern is nearly symmetric with a counterclockwise gyre north of the wind stress curl zero and clockwise south. The upper layer mean mass transport stream function is presented in Figure 1. The boundary conditions are free-slip everywhere. Meanders develop within the free jet and grow in time resulting eventually in eddy detachment.

2.2 Experiment E11

The applied wind stress is

$$\tau_x = \tau_m \cos(\frac{\pi}{L}(y - a)) \tag{2}$$

where $\tau_m = 2 \times 10^{-4} m^2 s^{-2}$, $L = 1000\,km$ and $a = 280\,km$. The resulting circulation pattern includes anticyclonic subtropical gyres in the Atlantic and Indian sectors, respectively, and an elongated cyclonic subpolar gyre south of the wind curl zero. Africa is represented by a

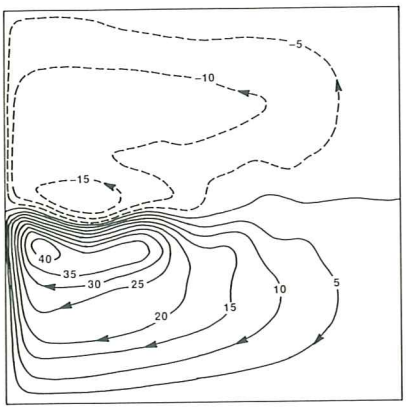

Figure 1: Upper layer mean mass transport stream function of 2G. The contour interval is 5 Sv.

triangular shape, approximating that of the Agulhas Bank shelf break. The upper layer mean mass transport stream function is shown in Figure 2. The boundary conditions are no-slip on meridional boundaries and free-slip on zonal boundaries. The intense boundary current along the eastern coast of Africa constitutes the Agulhas Current and the major part of it retroflects south of the tip of Africa, returning eastward toward the Indian Ocean. In turning back, several times a year the Agulhas intercepts itself and forms a ring which translates into the Atlantic. For more details on this experiment, the reader is referred to Boudra and Chassignet (1988) and Chassignet and Boudra (1988).

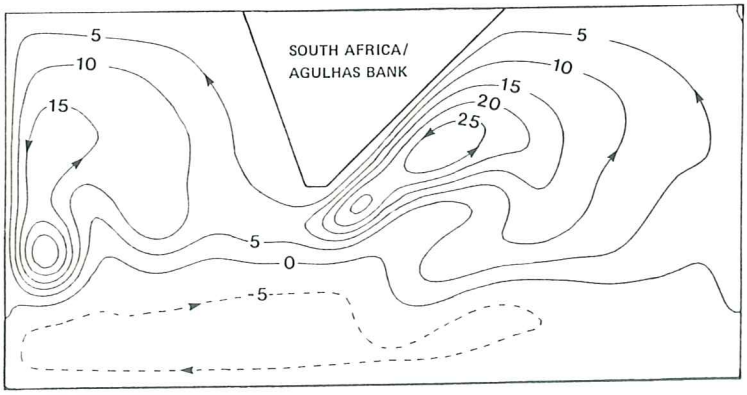

Figure 2: Upper layer mean mass transport stream function of E11. The contour interval is 5 Sv.

3 RING MOTION AND EVOLUTION

3.1 Description of the model rings 2G1 and 2G2

At day 6160 of the 7200 day double-gyre simulation (Figure 3a), a ring which we call 2G1

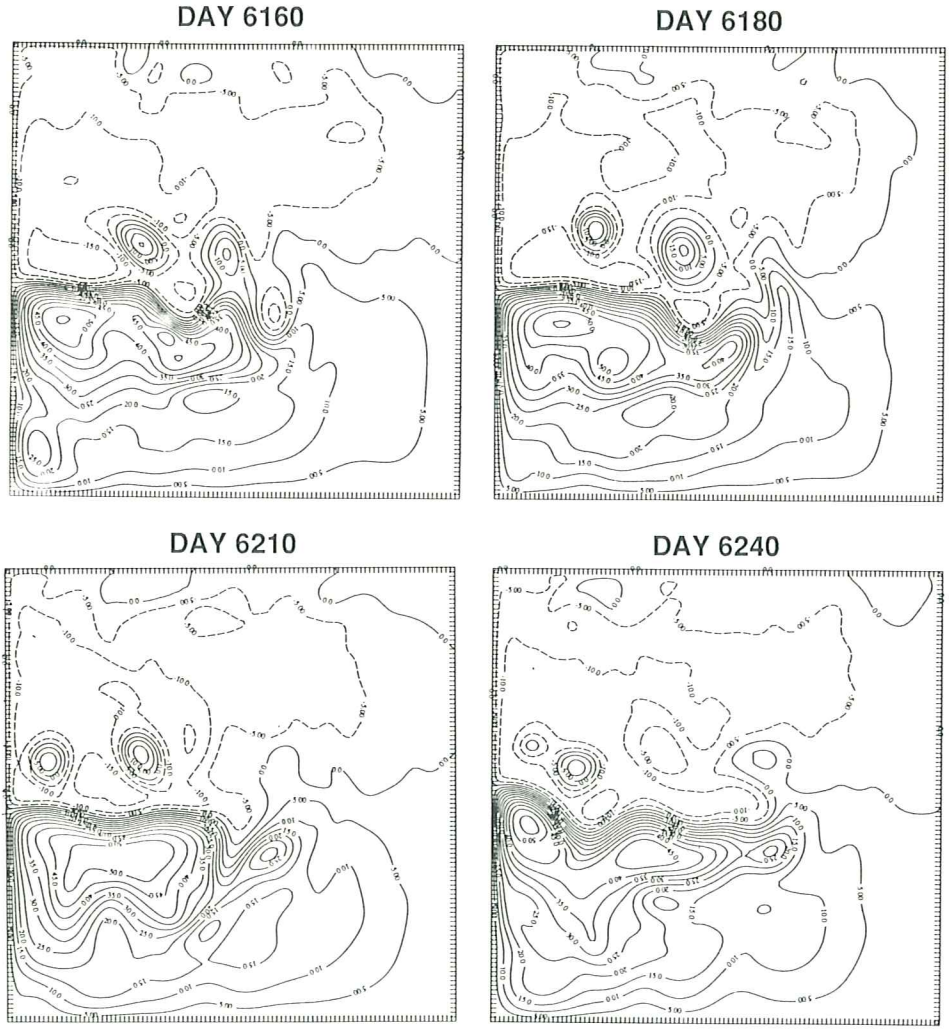

Figure 3: Time evolution of the upper layer mass stream function of 2G from day 6160 to day 6240. The contour interval is $5 \times 10^6 m^3 s^{-1}$.

has just separated from the free jet and a second ring (2G2) is forming. The time evolution of both rings is illustrated in Figure 3 for a period of 90 days. At day 6160, the shape of 2G1 is quite elongated and it is only at day 6180 (Figure 3b) that the ring becomes more symmetric. 2G1 keeps this quasi circular shape until day 6210 (Figure 3c) when the ring starts to interact with the western boundary of the basin. The propagation speed of 2G1 until day 6210 is approximately $9\,cm\,s^{-1}$ in the westward direction with a very small northward propagation. The ring 2G2 (Figure 3b) separates around day 6180 with a fairly circular shape and interacts with the free jet until day 6210. 2G2 moves westward at approximately the same speed as 2G1 until day 6240 (Figure 3d) where it encounters the now-weakened 2G1.

The diameters of the rings 2G1 and 2G2 just after formation are of approximately the same magnitude (250 to 300 km), their maximum velocities of the order of $60-80\,cm\,s^{-1}$ (2G2 and 2G1, respectively) at a radius of about $70\,km$ and a maximum interface displacement at the center of 250 to $300\,m$. In 50 days, the diameters and interface displacements at the center remain almost unchanged. There is first an increase in the maximum velocities to $100-120\,cm\,s^{-1}$ (2G2 and 2G1, respectively) followed by a decrease to $60-80\,cm\,s^{-1}$. Decay becomes important as soon as the rings reach the western boundary.

3.2 Description of the model ring RE11

The chosen ring RE11 formed around day 2950 (beginning of year 9 from a 10-year simulation) and the time evolution of its upper depth interface anomaly field is illustrated in Figure 4, for a period of 90 days. The ring formation process is described in detail in Chassignet and Boudra (1988). At day 2955 (Figure 4a), the ring has just separated from the Agulhas proper and moves in a southwestward direction. The shape is quite symmetric, but on its northern side some deformation occurs because of the presence of the African continent. As the ring rounds the tip of Africa, it is compressed between the continent and the return flow from the Atlantic basin. The ring's shape becomes elliptic and undergoes strong deformation as it propagates westward (Figure 4b,c,d). At day 3035 (Figure 4e), once the ring has escaped from the influence of Africa, it regains a more circular shape and starts to move toward the west-northwest. It then gets slowly absorbed by the South Atlantic subtropical gyre (Figure 4f). The propagation speed of the ring until day 3025 (when moving westward) is approximately $4.3\,cm\,s^{-1}$. The speed then increases to $6.2\,cm\,s^{-1}$ in the northwestward direction ($5.5\,cm\,s^{-1}$ toward the west and $2.8\,cm\,s^{-1}$ toward the north).

At day 2955, the ring diameter is of the order of 300 km, the maximum velocities of $120\,cm\,s^{-1}$ at a radius of about $80\,km$ and the interface displacement at center of $300\,m$. In 50 days, the diameter remains approximately unchanged, but the magnitude of the velocities has dropped by about 45% to $75\,cm\,s^{-1}$ and the interface displacement at the center to $260\,m$.

3.3 Comparisons with observations

(i) **Ring structures.** The physical structure of rings from various boundary currents around the world can be compared in a uniform manner through the use of a simple two-layer approximation of their first baroclinic structure. This approach is fully described in Olson *et*

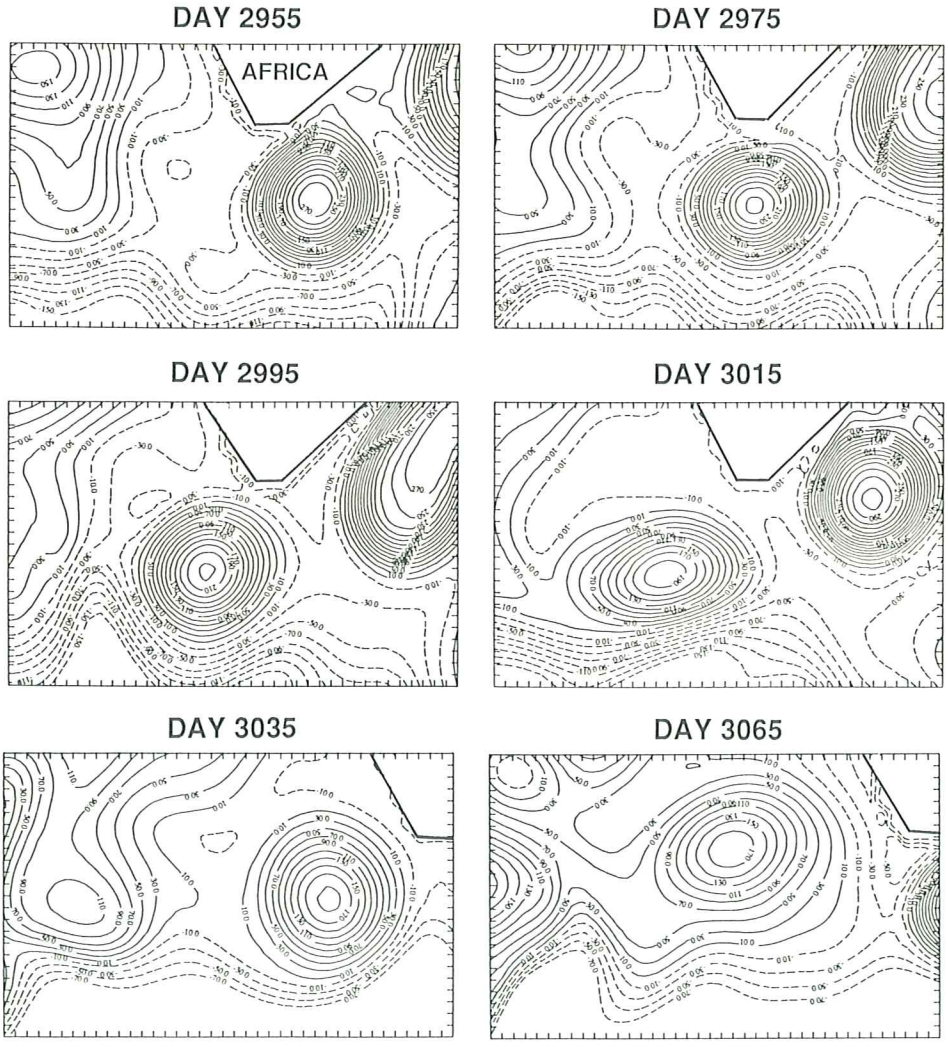

Figure 4: Time evolution of the upper depth interface anomaly field of RE11 from day 2955 to day 3065. The contour interval is 20 m.

al. (1985) who use as the interface the $10°C$ surface, thought to be a good approximation of the main thermocline of the ring. The model stratifications in the present study are chosen such that the upper layer thickness at rest gives a good representation of the mean thermocline depth in the domain (Table 1). Therefore, in order to make comparisons, the radial distribution of the depth of the first interface from the rings 2G1, 2G2 and RE11 and of the $10°C$ isotherm from Gulf Stream warm core ring 82B (Olson *et al.*, 1985) and two Agulhas rings surveyed in 1983 (Olson and Evans, 1986) are presented in Figure 5 and 6.

The first three profiles of 82B (March-June 1982) were taken when the ring was not interacting with the Gulf Stream, the last three when the ring was in contact (Figure 5a). Both 2G1 and 2G2 have a smaller interface displacement at the center (of the order of $50\,m$), but the major differences appear in ring diameter ($\sim 160\,km$ for 82B, 200 to $300\,km$ for 2G1 and 2G2) (Figure 5) and in volume (Table 2). 82B has velocity maxima between 30 and $70\,cm\,s^{-1}$ (between 60 and $120\,cm\,s^{-1}$ for 2G1 and 2G2) at a radius of about $50\,km$ ($70\,km$ for 2G1 and 2G2) (Olson *et al.*, 1985).

Differences between RE11 at day 2955 (just after formation when most vigorous) and the observed Agulhas rings (Figure 6) are a smaller interface depth of the model ring of 100 to $150\,m$ and less volume (Table 2). A better agreement between the model and observations might be obtained with a choice of a thicker upper layer ($400\,m$ at rest instead of $300\,m$ as in 2G) (Table 1) or of a shallower isotherm than $10°C$. Both observed rings have velocity maxima between 110 and $130\,km$ from center ($80\,km$ for RE11). The newer, southern ring (referred to as the Retrofection eddy in Table 2) is more intense, with maximum velocities of nearly $90\,cm\,s^{-1}$ (between 75 and $120\,cm\,s^{-1}$ for RE11) as compared to approximately $60\,cm\,s^{-1}$ in the northern ring (referred to as the Cape Town eddy) (Olson and Evans, 1986).

(ii) Ring translation speeds.

Gulf Stream rings were found by Brown *et al.* (1986) to have translation rates up to ten times faster than those expected for an equivalent upper layer isolated eddy from the theory of Nof (1981) and Flierl (1984).[2] Advection by the larger scale mean circulation and interactions with the Gulf Stream were suggested to account for the difference. Furthermore, this behavior is not restricted to Gulf Stream rings. Olson and Evans (1986) compared the translation speed of two Agulhas rings surveyed in Nov.-Dec. 1983 to Nof and Flierl's estimate. They found the observed translation rate to be approximately 2 to 5 times faster. This was attributed to advection by the larger scale flow.

The model rings (2G1, 2G2 and RE11) also exhibit this more rapid motion. Their propagation speeds are approximately of the same magnitude as their observed counterparts ($9\,cm\,s^{-1}$ for 2G1 and 2G2 to $6.5\,cm\,s^{-1}$ from long-lived Gulf Stream rings (Brown *et al.*, 1986); $6.2\,cm\,s^{-1}$ from RE11 to $4.8\,cm\,s^{-1}$ and $8.5\,cm\,s^{-1}$ from observed Agulhas rings (Olson and Evans, 1986)). Some of the factors affecting the rings propagation will be discussed in more detail in Section 4.

---

[2]These estimates are based on momentum integral over the ring $\left(c = \frac{-\beta}{2f} \frac{\iint h v r^2\, dr\, d\theta}{\iint (h - h_\infty)\, dr\, d\theta}\right)$ and are approximately equal to the long Rossby wave speed (Nof, 1981; Flierl, 1984).

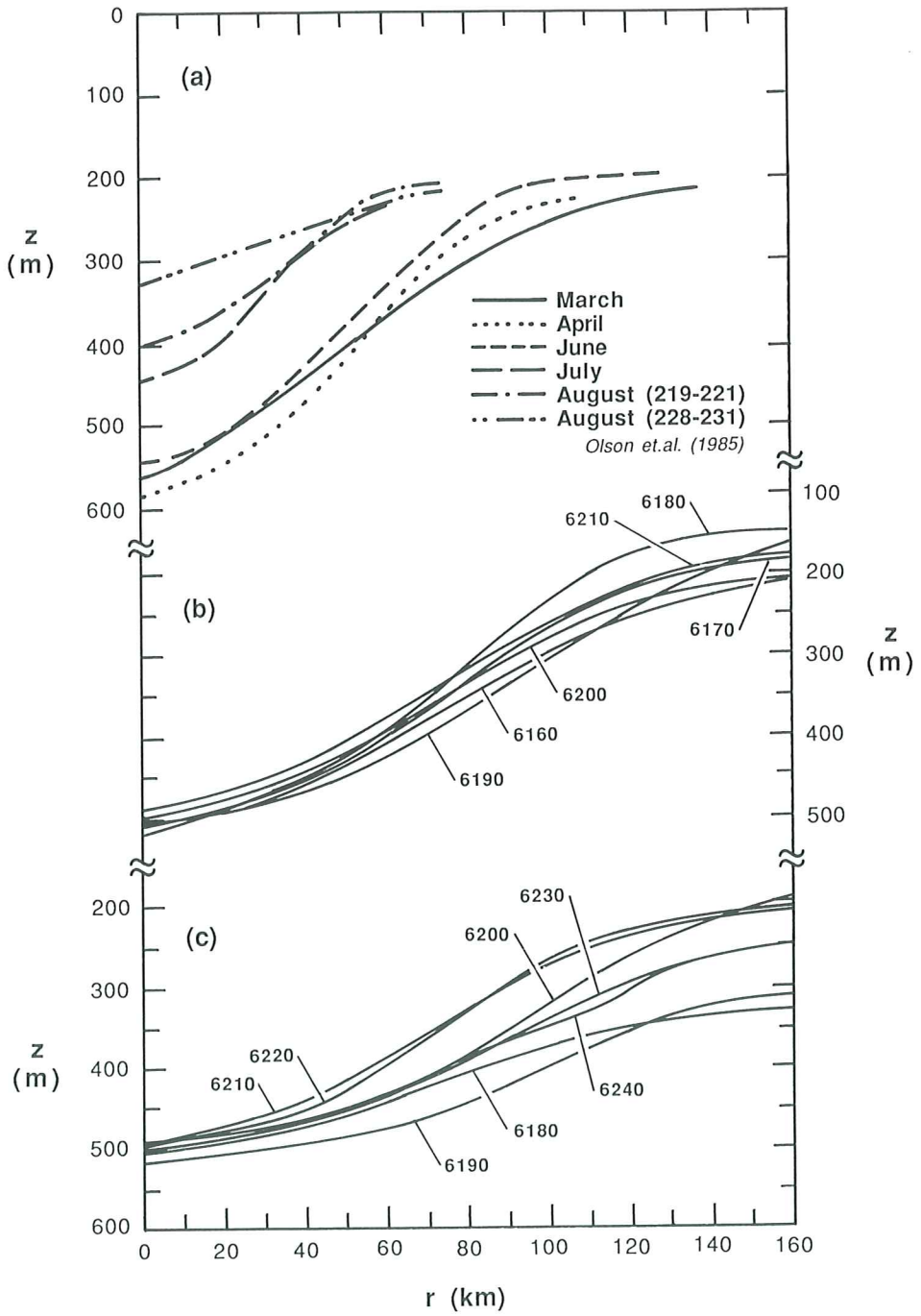

Figure 5: Radial distributions of the depth (a) of the $10°C$ isotherm from Gulf Stream warm core ring 82B (from Olson *et al.*, 1985) and of the first interface from (b) 2G1 (day 6160-6210) and (c) 2G2 (day 6180-6240).

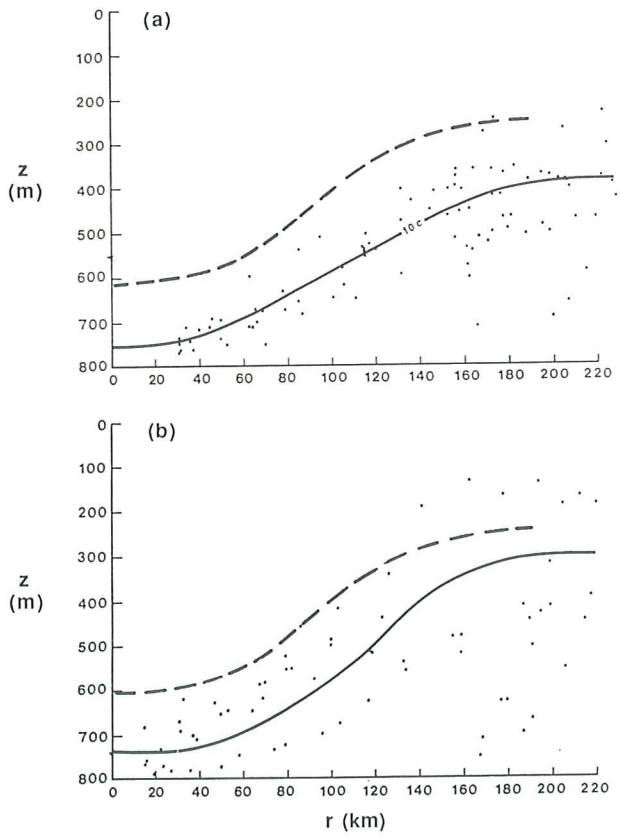

Figure 6: Radial distribution of the depth of the first interface from RE11 at day 2955 (dashed line) and of the $10°C$ isotherm (solid line) in (a) the northern and (b) the southern observed Agulhas rings (from Olson and Evans, 1986).

Ring	$P \times 10^{15} J$	$K \times 10^{15} J$	Vol. $\times 10^{12} m^3$
2G1	13.4	8.1	8.3
2G2	8.8	4.9	6.0
82B	4.2	1.0	3.9
RE11	11.2	8.5	8.3
Retroflection eddy	51.4	8.7	19.2
Cape Town eddy	30.5	6.2	15.2

Table 2: Available potential energy, kinetic energy and volume for 2G1 at day 6160, 2G2 at day 6210, Gulf Stream warm core ring 82B (Olson *et al.*, 1985), RE11 at day 2955 and two Agulhas rings (Olson and Evans, 1986).

(iii) Ring APE and KE. The depth of the $10°C$ isotherm is also used within the context of the two-layer model of the observed ring's structure (Olson *et al.*, 1985) to compute kinetic and available potential energy. The same calculation can be performed with the model rings by using the first interface depth (which corresponds approximately to that of the $10°C$ isotherm as shown previously). Upper layer kinetic energy (K_1), available potential energy associated with the first interface (P_1) and corresponding volume are calculated assuming the ring to be symmetric, which is not always the case as shown in section 3.1. Both 2G1 and 2G2 are more energetic than 82B (Table 2). On the other hand, the model Agulhas rings are smaller and less energetic than the two counterparts observed in Nov.-Dec. 1983 (Table 2).

Top layer decay time scales (τ_P, τ_K) for a certain period of time can be calculated by dividing the energy content of the ring by the time rate of change of each quantity over the time period. Model ring time decays ($\sim$ 100 days for both τ_P and τ_K) are found to be much faster than observed ones. In the case of the Gulf Stream ring 82B (Olson *et al.*, 1985), when the ring is outside the Gulf Stream and topographic influences, the τ_P decay scale is $\sim$ 500 days (compared to 600 and 520 days for cyclonic rings in the Sargasso sea (Olson, 1980)).

(iv) Gradient balance state. Once formed, the ring should evolve in time and reach an approximate gradient balance state

$$\frac{v^2}{r} + fv = g' \frac{\partial h}{\partial r}, \tag{3}$$

where v is the azimuthal velocity and $\frac{\partial h}{\partial r}$ the radial derivative of the interface depth h. Equation (3) is derived for a symmetric ring from the equations of motion for an inviscid fluid in a cylindrical coordinate system associated with the ring:

$$\frac{\partial u}{\partial t} + u\frac{\partial u}{\partial r} - \frac{v^2}{r} + \frac{v}{r}\frac{\partial u}{\partial \theta} + w\frac{\partial u}{\partial z} - fv = -\frac{1}{\rho}\frac{\partial p}{\partial r}, \tag{4}$$

$$\frac{\partial v}{\partial t} + \frac{vu}{r} + u\frac{\partial v}{\partial r} + \frac{v}{r}\frac{\partial v}{\partial \theta} + w\frac{\partial v}{\partial z} + fu = -\frac{1}{\rho r}\frac{\partial p}{\partial \theta}, \tag{5}$$

$$\frac{\partial w}{\partial t} + u\frac{\partial w}{\partial r} + \frac{v}{r}\frac{\partial w}{\partial \theta} + w\frac{\partial w}{\partial z} = -\frac{1}{\rho}\frac{\partial p}{\partial z} - g, \tag{6}$$

where u, v and w are the radial (r), azimuthal (θ) and vertical (z) velocities, respectively; p the pressure and ρ the density. If the ring is perfectly symmetric, $u = 0$ and then (3) is satisfied. If the ring is strongly out of balance, then the extra terms in (4) and (5) could start to play a significant role. Common practice for the scaling of rings is to consider the length scale L as the radius of maximum velocity and the velocity scale V as the maximum velocity V_{max} (Olson, 1980). If the ring is considered as consisting of two layers of fluid with different densities (Olson *et al.*, 1985), we can define a Burger number $B' = g' \frac{\Delta h}{f^2 L^2}$ for the change in interface height across the ring and the scaling of (3) leads to

$$R_o^2 + R_o = B', \tag{7}$$

where $R_o = \frac{V}{fL}$ is the Rossby number for the gradient flow. This scaling allows intercomparisons between different rings. R_o versus B' is represented in Figure 7. The dots in Figure 7a represent a compilation of 30 observed rings from the world ocean. The time evolutions of 2G1, 2G2, 82B and RE11 in the Rossby-Burger plane are represented in Figure 7b,c. 2G1, 2G2 and RE11 are well located among the majority of the world anticyclonic rings. On the other hand, Gulf Stream warm core ring 82B, 2G1 and 2G2 do not show a very organized pattern (Figure 7b), probably because of the presence of the near-by jet. At day 2955, RE11 is slightly off balance, but then adjusts and follows closely in time the scaled gradient balance curve (Figure 7c).

Olson *et al.* (1985) found that the direct surface velocity measurements of observed ring were consistently higher than those predicted by the gradient balance relation of (3) in a two-layer configuration, assuming the lower layer to be at rest. They suggested that the difference is due either to surface effects or to coherent barotropic modes. A similar result is obtained for RE11 even when the contribution of the second interface displacement is taken into account, the lower layer also being at rest. In this latter case, the upper layer gradient velocities are derived from

$$\frac{v_1^2}{r} + f v_1 = \frac{\partial}{\partial r}(g_1' h_1 + g_2' h_2), \tag{8}$$

where g_1', h_1, g_2' and h_2 correspond respectively to the reduced gravity and depth at the first and second interface and v_1 to the upper layer velocity. The corresponding velocity profile (model, gradient and geostrophic) of the upper layer of RE11 for day 2955 and day 3005 are displayed in Figure 8. The upper layer geostrophic velocity is computed as follows,

$$f v_{g_1} = \frac{\partial}{\partial r}(g_1' h_1 + g_2' h_2). \tag{9}$$

One can therefore ask to what extent is the approximation of a lower layer at rest valid. Equation (3) can be rewritten as

$$\frac{v^2}{r} + f v = f v_g, \tag{10}$$

where v_g is the total geostrophic velocity. For example, at day 2955 (Figure 8a), the observed maximum velocity in the upper layer is $v \sim 1.2 ms^{-1}$ and from (10), this leads to $v_g \sim$

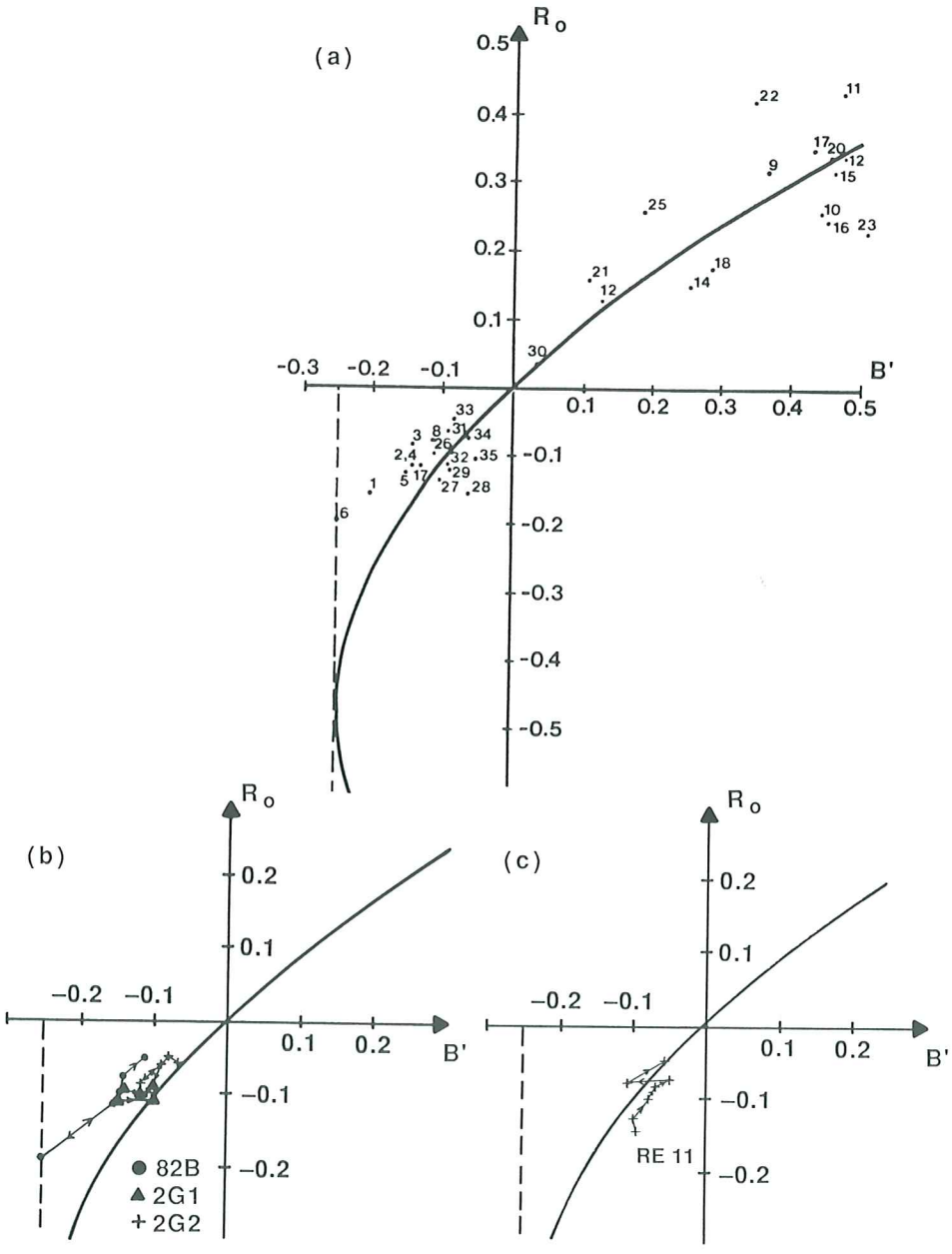

Figure 7: Representation of the Rossby number (R_o) for the gradient flow versus the Burger number (B') for the change in interface height across the ring. (a) Compilation of 30 world oceanic rings; (b) Evolution of Gulf Stream ring 82B, 2G1 and 2G2; (c) Evolution of RE11.

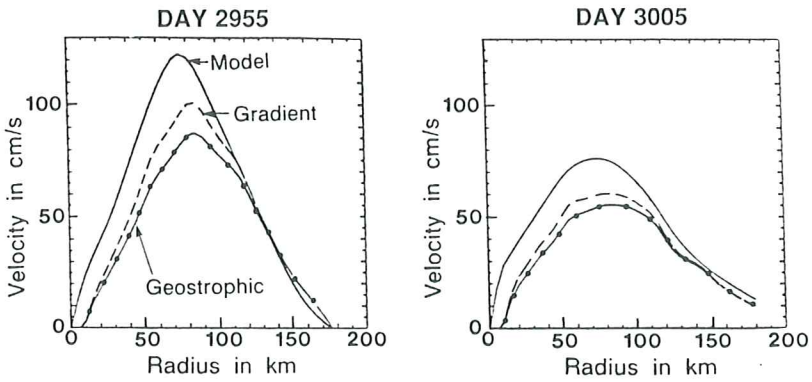

Figure 8: RE11 upper layer velocity profiles for day 2955 and day 3005 (Solid line for model velocities, dashed for gradient and dotted for geostrophic).

$1\,ms^{-1}$. The derived geostrophic velocity from Equation (9) is $\sim 0.85\,ms^{-1}$ (Figure 8) which implies velocities of the order of $0.15\,ms^{-1}$ in the lower layer to maintain the balance. This is effectively the case right underneath the ring. The same reasoning is valid for the other days. A similar calculation can be made for the two-layer model. The difference between the gradient velocities calculated assuming the lower layer at rest and the model velocities is the barotropic component of the flow. If the lower layer is considered to be at rest, the upper layer velocities of the ring are underestimated by about 10%. The model rings, therefore, have a coherent structure to the bottom. This may also be the case for observed rings since surface velocities are found to be higher than those predicted by the gradient balance assuming the lower layer at rest (Olson *et al.*, 1985; Olson and Evans, 1986). In fact, in the Agulhas case, vertically coherent structures (99%) of the flow (retroflection + rings) were recently found in two years of measurements with an array of current meter moorings south of Africa (Luyten, 1988, personal communication).

4 FACTORS AFFECTING THE RING MOTION AND EVOLUTION

In this section, only the specific case of RE11 is considered and the influence of several external factors on its propagation are investigated. In subsection 4.1, the model is first configured in the same basin as in section 2, but no wind stress is applied. The initial conditions are defined with the interface displacements and velocities of RE11. Then, in subsection 4.2, the African continent is removed to investigate the influence of its proximity on the ring propagation. The parameters used in each experiment are given in Table 3.

4.1 Ring R1 - Advection by the larger scale flows

In order to study the influence of the larger scale flows, first, the ring RE11 is extracted from E11 at day 2965. The position of the center was estimated and u, v and h in each layer within a radius of 150 km (distance from the center to the tip of Africa) were saved. The model

is then initialized with RE11 only and no wind forcing is applied. The initial conditions in the ring, referred now to as R1, are interface displacements and velocities of RE11 in each layer. The time evolution of R1 for a period of 200 days is illustrated in Figure 9. The ring is initially in contact with the African continent and generates a Kelvin wave along the eastern coast of Africa, leaving a strip of current behind it. This Kelvin wave propagates cyclonically around the basin (southern hemisphere). The measured wave speed is of the order of $2\,ms^{-1}$, which is between the first and second baroclinic mode Kelvin wave propagation speeds ($2.7\,ms^{-1}$ and $1.7\,ms^{-1}$, respectively, with $c_{Kelvin} = fR_d$).[3] As this pressure disturbance reaches the eastern boundary, it excites a wave whose western edge progresses at a speed of approximately $1.5\,cm\,s^{-1}$, which is of the order of the long Rossby wave speed βR_d^2, as expected ($1.5\,cm\,s^{-1}$ and $0.5\,cm\,s^{-1}$ for the first and second baroclinic modes, respectively).[3] Nof (1988) found that quasi-geostrophic eddies (*i.e.*, vortices with small amplitudes and weak circulation) on an f-plane, when in contact with a wall, leak fluid in a fashion similar to R1. Curiously, he also found that the leakage was completely blocked once the initialized eddy was at least weakly nonlinear. Comparisons are limited by the fact that Nof considers only upper-layer eddies with a lower layer at rest (reduced gravity model) and does not include the β-effect.

Because of the small basin size, the Kelvin wave can propagate around the entire basin and form a closed circulation (Figure 9c). The excitation of a Rossby wave at the eastern boundary, as a consequence of this Kelvin wave propagation, might also be linked to the generation of basin mode resonance. This was found to be important in the ring formation in a two-layer experiment with a rectangular Africa (Chassignet and Boudra, 1988).

The ring R1 initially moves westward until day 40 and northwestward thereafter, leaving behind it a Rossby wave wake (Flierl, 1977, 1984). It is only after day 150 (Figure 9f) that the ring detaches from the African continent. The propagation of R1 is almost directly westward during the first 40 days (Figure 9h) at a speed of $\sim 3.6\,cm\,s^{-1}$ (Table 4). This is close to the initial $4.3\,cm\,s^{-1}$ of RE11, nevertheless suggesting a small influence of the external flows on the propagation of RE11 during its passage from the Indian to the Atlantic basin. This

[3]The internal Rossby radii of deformation (R_d) are computed following Lighthill (1969) and assuming the at-rest stratification. Equivalent depth values of 74.2 and 27.4 *cm* are obtained for the two baroclinic modes, corresponding to radii (R_d) of 27 and 16 *km*, respectively.

Ring	Number of layers	Thickness of the layers (m)	g' (ms^{-2})	Bottom drag (s^{-1})	African continent (Yes or No)	Basin size $km \times km$	Initial conditions
R1	3	300	.02	10^{-7}	Yes	2520	Ring extracted from
		900	.005			×	E11, no wind forcing.
		3800				1280	
R2					No		As R1, but no Africa
	For all experiments, $\Delta x = 20\,km$.						

Table 3: Parameters of the experiments. Blanks indicate no change from the previous experiment.

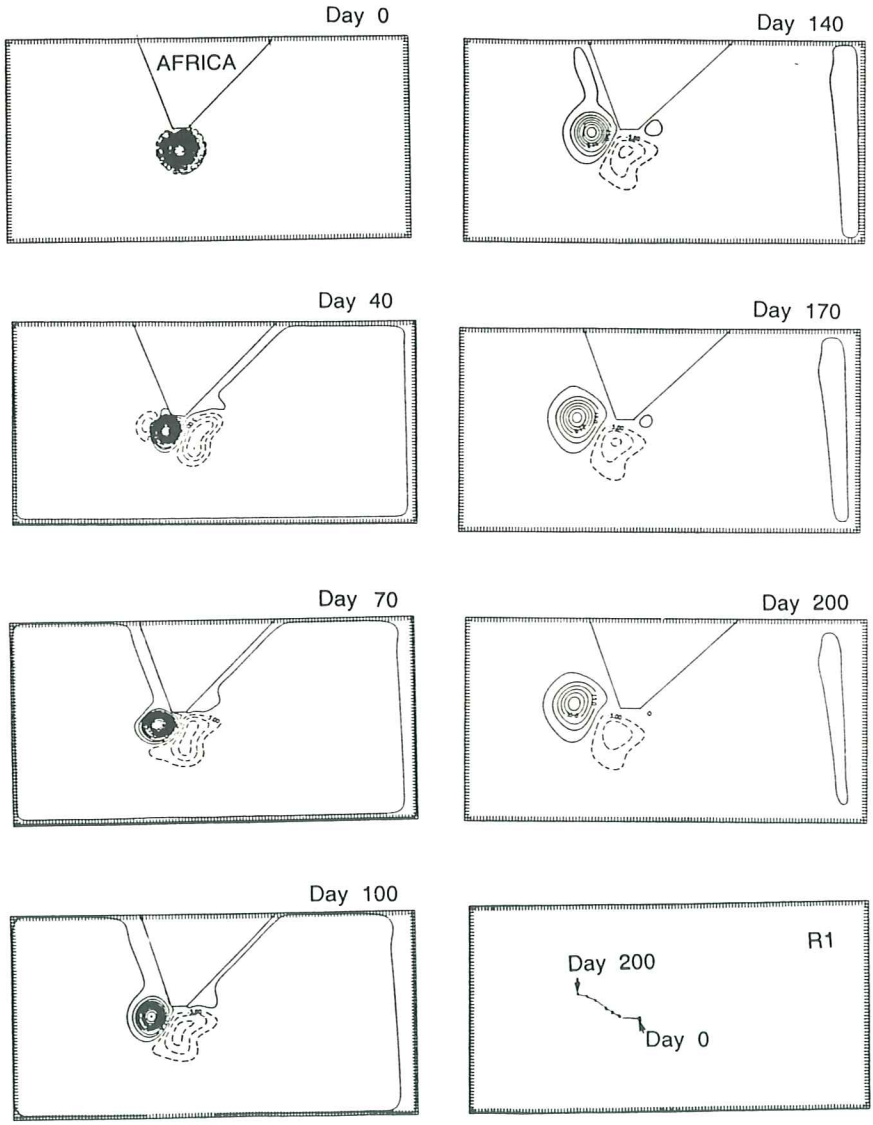

Figure 9: Upper layer interface displacement anomaly of R1 for a period of 200 days. The contour interval is 10 m.

Ring	c_{West} ($cm\,s^{-1}$)		c'_{North} ($cm\,s^{-1}$)		c_{Total} ($cm\,s^{-1}$)	
RE11	4.3	5.5	0	2.8	4.3	6.2
R1	3.6	1.9	0.4	1.1	3.8	2.2
R2	2.7	2.6	2.1	1.0	3.4	2.7

Table 4: Ring propagation speed. The first number in each column corresponds to the propagation speed averaged over the first 40 days, the second number to the propagation speed after the first 40 days.

is not surprising since there is almost no mean flow between the two basins. It is only when the ring rounds the tip of Africa that some leakage occurs between the ring and the African continent. After 40 days, R1 decelerates and moves northwestward at a speed $\sim 2.2\,cm\,s^{-1}$ (Table 4). This propagation speed is much slower than that of RE11 ($6.2\,cm\,s^{-1}$), suggesting a strong influence of the South Atlantic subtropical gyre on the movement of the latter.

4.2 Ring R2 - Influence of the African continent

In order to investigate the influence of the African continent, an experiment without Africa, R2, otherwise similar to R1, was run. Its time evolution is presented in Figure 10. The ring propagates in a northwestward direction, as expected from previous numerical studies (McWilliams and Flierl, 1979; Mied and Lindemann, 1979; Flierl, 1984) and also leaves behind a Rossby wave wake. This wake is of the same order of magnitude in size and intensity as for R1.

During the first 40 days, R2 propagates toward the west at a speed of the order of $2.7\,cm\,s^{-1}$ (Table 4), suggesting an influence from the African continent on the westward propagation speed of R1 of the order of $1\,cm\,s^{-1}$. The total speed of R2 for this period is $\sim 3.4\,cm\,s^{-1}$ (which is approximately equal to that of R1), with a northward component of $2.1\,cm\,s^{-1}$. This direction of motion (north) was not allowed in R1.

It is apparent that the presence of Africa in R1 influences the ring propagation and enhances the westward movement over that due to β. Sommerfeld (1950) showed that the interaction of a point vortex with a lateral boundary is analogous to the interaction of neighboring vortices of opposite sign. The analytical solutions which describe the resulting motion of two point vortices are well known and are a function of the circulation and the separation distance (Basset, 1888; Lamb, 1932; Sommerfeld, 1950; Batchelor, 1967). The problem becomes considerably more complex if the point sources are replaced by finite area vortices which allow the vortices to exchange mass (Hooker, 1987).

As described by Sommerfeld, the vortex is pushed forward by its virtual image obtained by reflection in the wall. This theory implies maximum velocities at the boundary and therefore is applicable in numerical models only when a free-slip boundary condition is used. When a no-slip condition is prescribed, this mirror image theory breaks down since the velocities

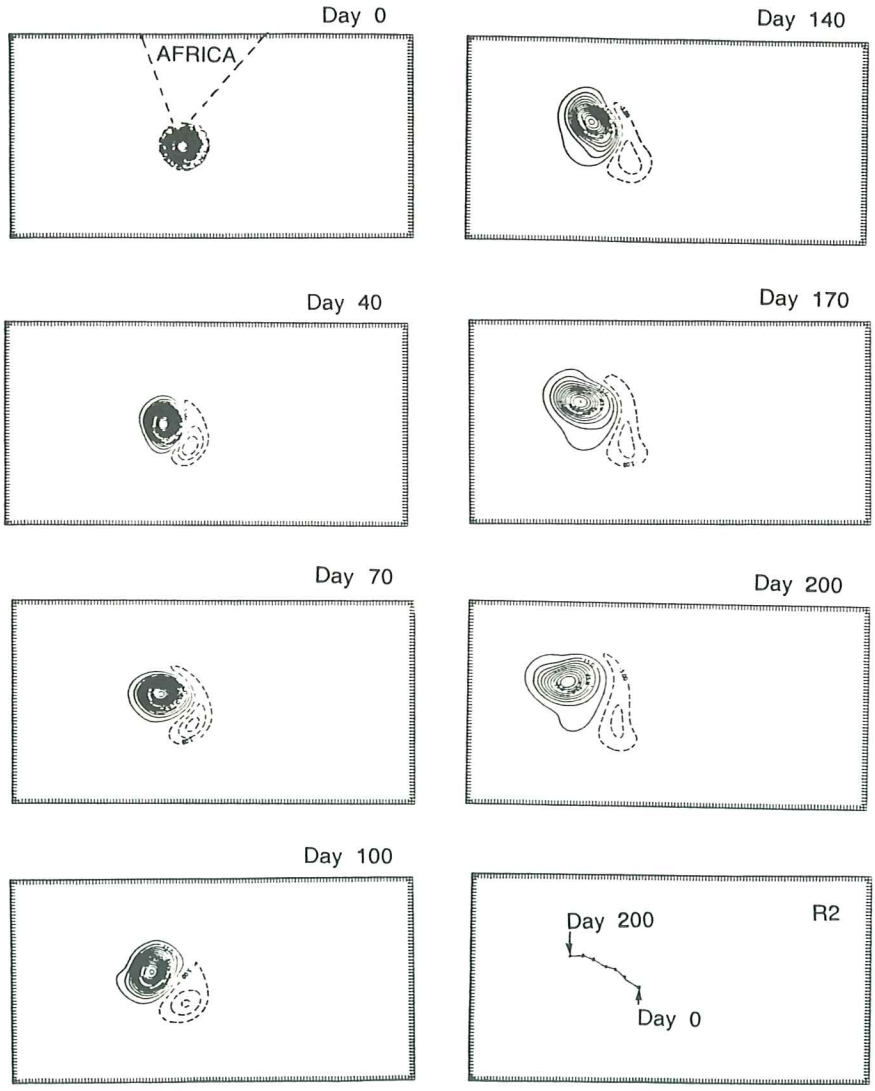

Figure 10: As in Figure 9 for R2.

have to be identically zero at the boundary. However, propagation along the wall in the same direction as for the effect of a virtual imge has been observed in numerical experiments using no-slip boundary conditions (Cox, 1979; Smith, 1986). Cox suggested that, by virtue of the no-slip condition, a narrow but intense band of vorticity of sign opposite to that of the eddy is present between the wall and the eddy and, considering the interactive effects of neighboring vortices (Sommerfeld, 1950; Hooker, 1987), this results in an alongshore movement of the eddy. It is surmised here that such an interaction may account for the differences between the propagation speeds of R1 and R2.

The westward propagation speed of R2 remains the same after the first 40 days, but the northward component decreases sharply, as if the initial period was one of adjustment to the environment (Table 4). Initially, most of the fluid is at rest and the only active force is due to β. In the absence of compensating pressure gradient forces, the stronger Coriolis force on the poleward versus the equatorward side will produce an equatorward force on an anticyclone, referred to as Rossby drift (Rossby, 1948; Holland, 1983). The ring will therefore experience an acceleration to the north. As compensating pressure forces develop, the motion is then turned to the west and the ring drifts westward in a circular analogy to the classical Rossby wave. Also, transient Rossby waves are generated which further influence the translation of the eddy, *i.e.* slow northward drift (*e.g.*, see Flierl, 1984).

5 SUMMARY AND DISCUSSION

Rings produced in a two-gyre wind driven circulation model (experiment 2G) and in a model of the South Atlantic/Indian Ocean (experiment E11) have been compared to observed Gulf Stream and Agulhas rings in a consistent fashion through the use of a diagnostic two-layer model. At this stage, especially the model vertical structure is still highly simplified with respect to reality as might be required to correctly simulate world ocean rings. Some attempt is made to begin to address this issue elsewhere in this volume (Boudra *et al.*, 1989). One also has to keep in mind that these comparisons have been carried out with only a limited number of rings, both observed and modeled. However, a good agreement is obtained between the observed rings' $10°C$ surface and the first interface depths of the modeled rings when the model mean upper layer thickness (approximation of the mean thermocline depth in the domain) is chosen to be $400\ m$. Therefore, some qualitative comparisons with reality can be made. The model and observed rings exhibit some substantial similarity in terms of thermocline depth, ring size, swirl velocities, and translation speeds, in addition to parameters such as the Rossby and Burger numbers. Direct surface velocity measurements in observed rings were found to be consistently higher than those predicted by the gradient balance assuming the lower layer to be at rest, and the same result was obtained for the model rings. In the model, it was demonstrated that this difference is due to the barotropic component of the flow, suggesting that the model rings have a coherent structure to the bottom. It seems likely that this is also the case for real oceanic rings.

One of the major differences between observed and model rings is in their decay rates. The decay rates of the model rings were found to be 4 to 6 times faster than in observed rings,

and are apparently strongly influenced by the lateral viscosity. McWilliams and Flierl (1979), in their study of quasigeostrophic isolated vortices, stated that the vortex amplitude decay rate, in the limit of strong nonlinearity, is governed by the frictional coefficient rather than dispersion. The question arises as to what extent the decay is due to Rossby wave radiation (horizontal and vertical) in the above rings. In the case of an inviscid upper layer lens in the same parameter range as one of those studied here (RE11), Flierl (1984) found a decay of the order of 7 years ($\sim$ 2500 days) due to Rossby wave radiation in the lower layer. This is at least one order of magnitude slower than the decay rates obtained in the model. Thus, it seems most likely that, as in McWilliams and Flierl (1979), viscous effects are the predominant energy sink. It is felt that the use of a lateral viscosity of 50 to 100 $m^2 s^{-1}$ (instead of the current 330 $m^2 s^{-1}$) might bring about comparable decay times between the modeled and observed rings. In the framework of this numerical model, such small viscosities could be employed only with a reduction in grid spacing to perhaps one-half the current 20 km.

A successful intercomparison between observed and modeled rings provides the opportunity and justification to isolate the factors in the model influencing the ring motion and evolution, which is not possible with observations alone. This has been carried out by examining in some detail the motion and evolution of one E11 ring and comparing with the behavior of a similar ring in each of several subsidiary experiments. It is found that the presence of Africa provides a westward motion in addition to that due to β, and it seems that this owes to interaction between the ring and a high vorticity band along the no-slip boundary. This topic deserves further investigation in a study focused on eddy-wall interaction. There is apparently only a small influence from the external flows on the propagation of the ring during its passage from the Indian to the Atlantic basin. There is no continual flow between the two basins. It is only when the ring rounds the tip of Africa that a leakage is observed between the ring and the African continent. The advection by the large scale flows is found to dominate the motion once the ring drifts into the South Atlantic subtropical gyre.

On the one hand, the relative simplicity of the model allowed the possibility to analyze some of the physical mechanisms behind ring propagation, such as advection by the mean flow or boundary influence. On the other, the effects of bottom topography/realistic coastline are also felt to be of importance, and the model's simplicity has, thus far, inhibited their determination. It is, therefore, expected that more insight into ring propagation and evolution can continue to be gained as the realism/complexity of the models is further increased.

6 ACKNOWLEDGEMENTS

This work was supported by NSF grants OCE-8502126 and OCE-8600593 and by the Office of Naval Research grant No. N00014-87-G0116. Computations were carried out using the CRAY computers at the National Center for Atmospheric Research (NCAR). NCAR is sponsored by the National Science Foundation.

7 REFERENCES

Basset, A.B., 1888: *A treatise on hydrodynamics.* Dover Publications, **2:** 328 pp.

Batchelor, G.K., 1967: *An introduction to fluid dynamics.* Cambridge University Press, 615 pp.

Bleck, R. and D.B. Boudra, 1981: Initial testing of a numerical model ocean circulation

model using a Hybrid (quasi-Isopycnic) vertical coordinate. *J. Phy. Oceanogr.*, **11**, 755-770.

Boudra, D.B. and E.P. Chassignet, 1988: Dynamics of Agulhas retroflection and ring formation in a numerical model. Part I. The vorticity balance. *J. Phys. Oceanogr.*, **18**, 280-303.

Boudra, D.B., K.A. Maillet, and E.P. Chassignet, 1989: Numerical modeling of Agulhas retroflection and ring formation with isopycnal outcropping. In *Mesoscale Synoptic Coherent Structures in Geophysical Turbulence.* J.C.J. Nihoul and B.M. Jamart, Eds. Elsevier, Amsterdam. Submitted.

Brown, O.B., P.C. Cornillon, S.R. Emmerson and H.M. Carle, 1986: Gulf Stream warm rings: A statistical study of their behavior. *Deep-Sea Res.*, **33**, 1459-1473.

Chassignet, E.P. and D.B. Boudra, 1988: Dynamics of Agulhas retroflection and ring formation in a numerical model. Part II. Energetics and ring formation. *J. Phys. Oceanogr.*, **18**, 304-319.

Cheney, R.E. and P.L. Richardson, 1976: Observed decay of a cyclonic Gulf Stream ring. *Deep-Sea Res.*, **23**, 143-155.

Cox, M.D., 1979: A numerical study of Somali Current eddies. *J. Phys. Oceanogr.*, **9**, 312-326.

Flierl, G.R., 1977: The application of linear quasigeostrophic dynamics to Gulf Stream rings. *J. Phys. Oceanogr.*, **7**, 365-379.

Flierl, G.R., 1984: Rossby wave radiation from a strongly nonlinear warm eddy. *J. Phys. Oceanogr.*, **14**, 47-58.

Holland, G.J., 1983: Tropical cyclone motion: Environmental interaction plus a beta effect. *J. Atmos. Sci.*, **40**, 328-342.

Hooker, S.B., 1987: *Mesoscale eddy dynamics by the method of point vortices.* Ph.D. Thesis, University of Miami, 158 pp.

Lamb, H., 1932. *Hydrodynamics.* 6th ed. Cambridge University press, 738 pp.

Lighthill, M.J., 1969: Linear theory of long waves in a horizontally stratified ocean of uniform depth (Appendix). *Philos. Trans. R. Soc. London*, **265**, 85-92.

McWilliams, J.C. amd G.R. Flierl, 1979: On the evolution of isolated non-linear vortices, with application to Gulf Stream rings. *J. Phys. Oceanogr.*, **9**, 1155-1182.

Mied, R.P. and G.J. Lindemann, 1979: The propagation and evolution of cyclonic Gulf Stream rings. *J. Phys. Oceanogr.*, **9**, 1183-1206.

Nof, D., 1981: On the β-induced movement of isolated baroclinic eddies. *J. Phys. Oceanogr.*, **11**, 1662-1672.

Nof, D., 1988: Eddy-wall interactions. *J. Mar. Res.*, **46**, 527-555.

Olson, D.B., 1980: The physical oceanography of two rings observed by the cyclonic ring experiment. II. Dynamics. *J. Phys. Oceanogr.*, **10**, 514-528.

Olson, D.B., R.W. Schmitt, M. Kennelly and T.M. Joyce, 1985: A two-layer diagnostic model of the long-term physical evolution of warm-core ring 82B. *J. Geophys. Res.*, **90**, 8813-8822.

Olson, D.B. and R.H. Evans, 1986: Rings of the Agulhas. *Deep-sea Res.*, **33**, 27-42.

Rossby, C.G., 1948: On displacements and intensity changes of atmospheric vortices. *J. Mar. Res*, **7**, 175-187.

Sommerfeld, A., 1950: *Mechanics of deformable bodies.* Academic Press, New York, 396 pp.

Smith, D.C, IV, 1986: A numerical study of Loop Current eddy interaction with topography in the western Gulf of Mexico. *J. Phys. Oceanogr.*, **16**, 1260-1272.